World Academy of Science, Engineering and Technology
International Journal of Mechanical and Mechatronics Engineering
Vol:9, No:11, 2015

Time-Frequency Modeling and Analysis of Faulty Rotor

B. X. Tchomeni, A. A. Alugongo, T. B. Tengen

***Abstract*—**In this paper, de Laval rotor system has been characterized by a hinge model and its transient response numerically treated for a dynamic solution. The effect of the ensuing non-linear disturbances namely rub and breathing crack is numerically simulated. Subsequently, three analysis methods: Orbit Analysis, Fast Fourier Transform (FFT), and Wavelet Transform (WT) are employed to extract features of the vibration signal of the faulty system. An analysis of the system response orbits clearly indicates the perturbations due to the rotor-to-stator contact. The sensitivities of WT to the variation in system speed have been investigated by Continuous Wavelet Transform (CWT). The analysis reveals that features of crack, rubs and unbalance in vibration response can be useful for condition monitoring. WT reveals its ability to detect non-linear signal, and obtained results provide a useful tool method for detecting machinery faults.

***Keywords*—**Continuous wavelet, crack, discrete wavelet, high acceleration, low acceleration, nonlinear, rotor-stator, rub.

I. Introduction

UNTIL the 1980s research on vibration condition monitoring focused on determination of rotor Eigen modes, critical speeds and the prediction of response amplitudes of rotors subjected to an unbalance [1]. In order to obtain more realistic predictions; there is need for research and improvement in simulation models and numerical methods used to analyse rotor dynamic problems. The use of these different tools of analysis requires a better understanding of the physical phenomena involved.

Classical analysis of models using a Jeffcott rotor has been proposed by various researchers [2]. Those model prototypes have revealed an integration of various faults in order to predict all the possibilities of damages detectable on the machine. The Gasch's model has been adopted in several papers, which consider a cracked rotor running at a constant speed [2]. Dimaragonas et al. derived a rough analytical estimate of a crack compliance based on the energy principle proposed by [3], [4]. Friswell et al. proposed [5] a method that can reliably estimate both the rotor unbalance and misalignment from a single machine run-down. Sekhar and Prabhu performed a transient analysis on a cracked rotor passing through critical speed [6]. More recently, Tchomeni et al. adopted in [7], the views in [8], [9] to investigate the lateral and torsional vibration of four degree of freedom rotor stator with multiple parametric excitations for high speed. This model yields a better understanding of the rotor condition monitoring strategies based on the energy principle. Sinou experimentally investigated the possibility of detecting an open crack in rotating machinery for low or high rotor acceleration [10]. His studies considered the dynamic transient signals of a notched rotor by both Fast Fourier Transform (FFT) and Continuous Wavelet Transform (CWT). His works reveal that difficulties in identifying non-stationary vibration signals of the rotor with an open transverse crack at high accelerations can significantly be overcome by using advanced multiresolution spectral analysis techniques.

Wavelet Transform (WT) has been used in [11] to investigated the detection and monitoring of cracks in a rotor-bearing system. Wigner-Ville Distribution (WVD) and WT have been used in [12] to simulate the transient response of an accelerated cracked Jeffcott rotor with a switching crack and its time-frequency features. However, further investigations are needed in order to demonstrate the effectiveness and reliability of this new method in crack detection.

This paper focuses on using CWT to present the feasibility of these applications to diagnose the non-stationary vibration signals for high acceleration of the rotating rotor. Finally, two approaches regarding the detection and monitoring of the rotor are examined. The first uses the conventional FFT to analyse steady-state signal vibration of the rotor; the second, uses wavelet transforms to provide diagnosis of non- stationary transient signal of the rotor with high acceleration. The effectiveness of CWT in some cases in which the FFT fails to provide results for rub, crack disturbance are illustrated in various simulated tests.

II. Model of Study and Numerical Simulation

Consider Fig. 1 (a) in which a de Laval rotor of disc mass m supported on a massless elastic shaft of length L with a transverse crack near the disc in the inertial coordinates (X, Y) and rotating coordinates system (ξ,η). Let the disc be located mid-span with sliding bearings support at each end. Given a uniform rotary motion with constant angular velocity ω_0 and weight dominance, the system dynamic equation can be written in the form [12]:

$$\begin{bmatrix} m & 0 \\ 0 & m \end{bmatrix}\begin{pmatrix} \ddot{X} \\ \ddot{Y} \end{pmatrix}+\begin{bmatrix} c & 0 \\ 0 & c \end{bmatrix}\begin{pmatrix} \dot{X} \\ \dot{Y} \end{pmatrix}+\begin{bmatrix} k_x & k_{xy} \\ k_{yx} & k_y \end{bmatrix}\begin{pmatrix} X \\ Y \end{pmatrix}=\begin{pmatrix} f_X \\ f_Y \end{pmatrix}+\begin{pmatrix} mg \\ 0 \end{pmatrix}+\begin{pmatrix} F_X \\ F_Y \end{pmatrix} \quad (1)$$

where c, k, f, F are respectively, damping coefficient, the stiffness coefficient, and external disturbance.

B. X. Tchomeni and A. A. Alugongo are with the Vaal University of Technology, Vanderbijlpark, South Africa (Phone:+27- 169509302; fax: +27-169509797; e-mail: bmignon@ gmail.com,alfayoa@vut.ac.za).

T.B. Tengen, is with Ind. Eng Dept., Vaal University of Technology, Vanderbijlpark, South Africa (Phone: +27- 169506817; fax: +27-169509797; e-mail: thomas@vut.ac.za).

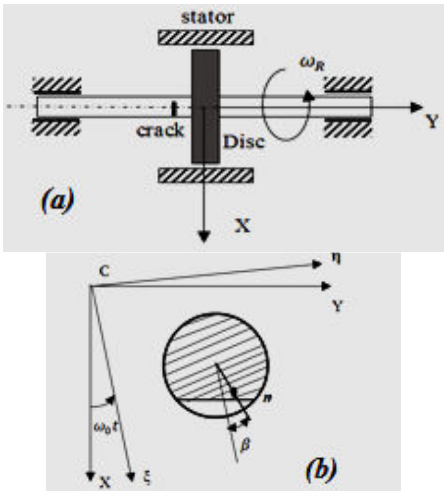

Fig. 1 (a) Model of rotor-sliding bearing in rub, (b) Coordinate system of the cracked rotor and disc unbalance

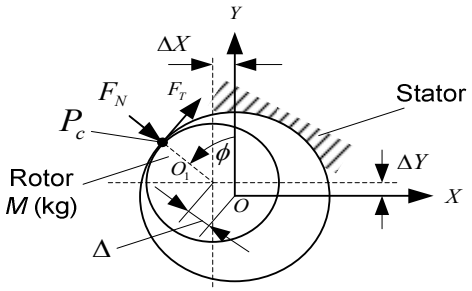

Fig. 2 Geometry of rotor, rubbing impact force and a clearance

III. Forces Acting on the Rotor's Shaft

Let Δ, M, R_d, and ω respectively be, rotor-stator static clearance, mass, radius and angular velocity of the disc about O, as shown in Fig. 2. On touching the stator, the rotor rubs on or bounces on, exciting vibration of the ring and rotor shaft. The shaft deflects due to, torque, crack and unbalance. A friction forceF_T, acts against rotation at the contact point.

Referring to Fig. 2, the position of the shaft center and rotor-stator clearance are, $\vec{R} = X\vec{\imath} + \overrightarrow{Yj}$, and $\Delta = R_r - R_s$. A friction force F_T, acts against rotation at the contact point P_c. Impact occurs when,

$$R - \Delta \geq 0 \tag{2}$$

when $R < \Delta$, the contact ceases and the friction force vanishes. The value of R at an arbitrary point P_c, is

$$R = \sqrt{(X - \Delta X)^2 + (Y - \Delta Y)^2}. \tag{3}$$

The position of P_c relative to point O in the (X, Y) frame is given by,

$$\vec{R} = (\Delta + \Delta_{XY})(cos\theta\vec{\imath} + sin\theta\vec{j}) \tag{4}$$

where

$$\begin{cases} X = (\Delta_X + \Delta)cos\theta \\ Y = (\Delta_Y + \Delta)sin\theta \end{cases} \tag{5}$$

and

$$tan\emptyset = \frac{Y}{X} \tag{6}$$

From the geometry of Fig. 2, and the above discussion,

$$\begin{cases} F_N = K_s(R - \Delta) \\ F_T = -\mu K_s(R - \Delta) \end{cases} \tag{7}$$

where, F_N and μ respectively are, radial component due to impact and friction coefficient. The lateral forces in both $X$and Y directions are:

$$F_X = -F_N cos\theta + F_T sin\theta;$$

$$F_Y = -F_N sin\theta - F_T cos\theta \tag{8}$$

In Cartesian coordinates, the forces are expressed as [9]:

$$\begin{cases} F_{1X} = -K_s\left(1 - \frac{\Delta}{R}\right)X + K_s\left(1 - \frac{\Delta}{R}\right)\mu Y \\ F_{1Y} = -K_s\left(1 - \frac{\Delta}{R}\right)\mu X - K_s\left(1 - \frac{\Delta}{R}\right)Y \end{cases} \tag{9}$$

IV. Crack Model and Stiffness Matrix

The inertial frame may be mapped to the rotational frame by the transformation.

$$\mathbf{T} = \begin{bmatrix} \cos\theta & \sin\theta \\ -\sin\theta & \cos\theta \end{bmatrix} \tag{10}$$

where, $\theta = \frac{1}{2}a_1 t^2 + \omega_0 t$. The stiffness matrix in the rotational frame is

$$\begin{bmatrix} k_\xi & 0 \\ 0 & k_\eta \end{bmatrix} = \begin{bmatrix} k_X & 0 \\ 0 & k_Y \end{bmatrix} - f(\theta)\begin{bmatrix} \Delta k_\xi & 0 \\ 0 & 0 \end{bmatrix} \tag{11}$$

where, k_ξ, k_η are respectively, the stiffness in the ξ-axis direction, and the stiffness in the η -axis direction. k_X is the stiffness of the non-cracked rotor ($k_X = k_Y$), Δk_ξ is the stiffness variation in the ξ-axis direction. For weight dominant vibrations, the modified function $f(\theta)$ for crack closure and opening is:

$$f(\theta) = \begin{cases} 1 & 2k\pi \leq \theta < (2h + \frac{1}{2})\pi \quad the\ crack\ is\ open \\ 0 & (2h + \frac{1}{2})\pi \leq \theta < (2h + \frac{3}{2})\pi \quad the\ crack\ is\ closed \\ 1 & (2h + \frac{3}{2})\pi \leq \theta < (2h + 2)\pi \quad the\ crack\ is\ open \end{cases} \tag{12}$$

where, $h = 0,1,2,\cdots$, $\theta(t) = \frac{1}{2}a_1 t^2 + \omega_0 t + \beta$, a_1, ω_0, β are the angular acceleration, initial angular speed, the angle of the unbalance with respect to the ξ axis.

When Fourier transformed, the modified open-closure function changes to:

$$f(\theta) = \frac{1}{2} + \frac{2}{\pi}\sum_{n=1}^{h}(-1)^n \frac{\cos(2n-1)\theta}{(2n-1)} \tag{13}$$

where the nth term of the cosine series in the Fourier expansion is $\frac{\cos(2n-1)\theta}{(2n-1)}$ and h is the number of terms that contain the cosine in the summed series.

The stiffness matrix in the inertial frame assumes the following form:

$$\begin{bmatrix} k_{XX} & k_{XY} \\ k_{YX} & k_{YY} \end{bmatrix} = \mathbf{T}^{-1}\begin{bmatrix} k_\xi & 0 \\ 0 & k_\eta \end{bmatrix}\mathbf{T} = \begin{bmatrix} k_0 & 0 \\ 0 & k_0 \end{bmatrix} - \frac{1}{2} f(\theta)\Delta k_\xi \begin{bmatrix} 1+\cos 2\theta & \sin 2\theta \\ \sin 2\theta & 1-\cos 2\theta \end{bmatrix} \tag{14}$$

The unbalance forces, f_x, f_y are

$$\begin{pmatrix} f_x \\ f_y \end{pmatrix} = me\begin{pmatrix} \ddot{\theta}\sin\theta + \dot{\theta}^2\cos\theta \\ -\ddot{\theta}\cos\theta + \dot{\theta}^2\sin\theta \end{pmatrix} \tag{15}$$

where e is the disc mass eccentricity. Under the stated conditions, the following approximation is adopted [12]:

$$\begin{pmatrix} x \\ y \end{pmatrix} \approx \begin{pmatrix} x \\ y \end{pmatrix}_{st} = \begin{pmatrix} \frac{mg}{k_x} \\ 0 \end{pmatrix} = \begin{pmatrix} x_{st} \\ 0 \end{pmatrix} \tag{16}$$

Substituting the stiffness matrix from (14) into (1) and introducing the angular acceleration, $\theta(t)$,the crack excitation, unbalance forces, friction, and gravitational forces including the angular acceleration terms in inertial coordinate frame read as:

$$\begin{bmatrix} m & 0 \\ 0 & m \end{bmatrix}\begin{pmatrix} \ddot{X} \\ \ddot{Y} \end{pmatrix} + \begin{bmatrix} c & 0 \\ 0 & c \end{bmatrix}\begin{pmatrix} \dot{X} \\ \dot{Y} \end{pmatrix} + \begin{bmatrix} k_0 & k_{xy} \\ k_{yx} & k_0 \end{bmatrix}\begin{pmatrix} X \\ Y \end{pmatrix} = \frac{1}{2} f(\theta)\Delta k_\xi \begin{bmatrix} 1+\cos 2\theta & \sin 2\theta \\ \sin 2\theta & 1-\cos 2\theta \end{bmatrix}\begin{pmatrix} x_{st} \\ 0 \end{pmatrix} + me\begin{pmatrix} \ddot{\theta}\sin\theta + \dot{\theta}^2\cos\theta \\ -\ddot{\theta}\cos\theta + \dot{\theta}^2\sin\theta \end{pmatrix} + \begin{pmatrix} F_{1X} \\ F_{2Y} \end{pmatrix} \tag{17}$$

where the second terms on the right side of (17) are respectively the crack excitation, unbalance excitation force and rubbing forces.

V. Numerical Simulation and Wavelet Transform

A classical Runge-Kutta algorithm has been used to obtain a dynamic response in which the weight is neglected in order to annul the influence of the static component of the response due to the weight on time-frequency features of the rotor. The values of the rotor properties for the transient analysis are adopted from [8] as: $m = 51.0\,kg$, $\Delta t = 0.001\,s$, $W_{stat} = 0.5\,mm$, $e = 0.01mm$ shaft stiffness and stator stiffness:

$$k_0 = 9.99 \times 10^5 \frac{N}{m}, \quad k_s = 5 \times \frac{10^8 N}{m},$$
$$D = d/2m\omega_0 = 0.1, \quad \omega_0 = (g/W_{stat})^{0.5},$$
$$a_1 = 15\,rad/s^2,$$
$$\Delta k_\xi = 0.95,$$

The coefficient of friction: $\mu = 0.25$.

The numerical integration of (17) is carried out in step-wise variations in stiffness represented by converging Fourier series with four terms as given by (13). The dynamic responses of rotor passing through the critical speed with unbalance, rub force are evaluated under the effect of the crack disturbance.

VI. Wavelet Transform

Signal analysis by the wavelet technique has progressively increased since1995. Wavelet transform is an effective tool in vibration study, signal, and numerical analysis [13].

Wavelet time-frequency transform is a multi-resolution analysis algorithm and is the inner product of the signal and a family of the wavelet. For the mother wavelet or the wavelet prototype $\psi(t)$, there exists a corresponding family of wavelet (son wavelet). The series of the son wavelets are generated by dilation and translation from the mother wavelet, $\psi(t)$ as [14]:

$$\psi_{a,b}(t) = \frac{1}{\sqrt{|a|}}\psi\left(\frac{t-b}{a}\right) \tag{18}$$

where, a and b are dilation (scaling) and translation (shift) parameters respectively. The factor $|a|^{-1/2}$ is used to ensure energy preservation. $\psi(t)$ is a square integral complex function, satisfying the admissibility condition [14].

$$c_\psi = \int_{-\infty}^{+\infty} \frac{|\psi(\omega)|^2}{|\omega|} d\omega < \infty \tag{19}$$

$\psi(\omega)$ is the Fourier transform of $\psi(t)$.

The continuous wavelet time-frequency transform of the initial signal $s(t)$ is expressed as:

$$CWT_s(a,b) = \int s(t)\cdot\psi^*_{a,b}(t)dt \tag{20}$$

where $\psi^*_{a,b}(t)$ is the complex conjugate function of $\psi_{a,b}(t)$.

By varying a and b, the wavelet time-frequency transform coefficients $W_s(a,b)$ can offer the representation of the signal $s(t)$ at different levels of resolution and time shift. In the process, thus, the wavelet time-frequency transform enables one to extract features of the signal $s(t)$.

VII. Application, Results and Discussions

Initially, the dynamic response of the unbalanced, uncracked system without, rubs is simulated numerically. Further, a crack,

Figs. 3 (a)-(c) show vibrations in X direction, the orbits patterns and the frequency spectrum of the rotor without, a crack and rubs while passing through first critical speed.

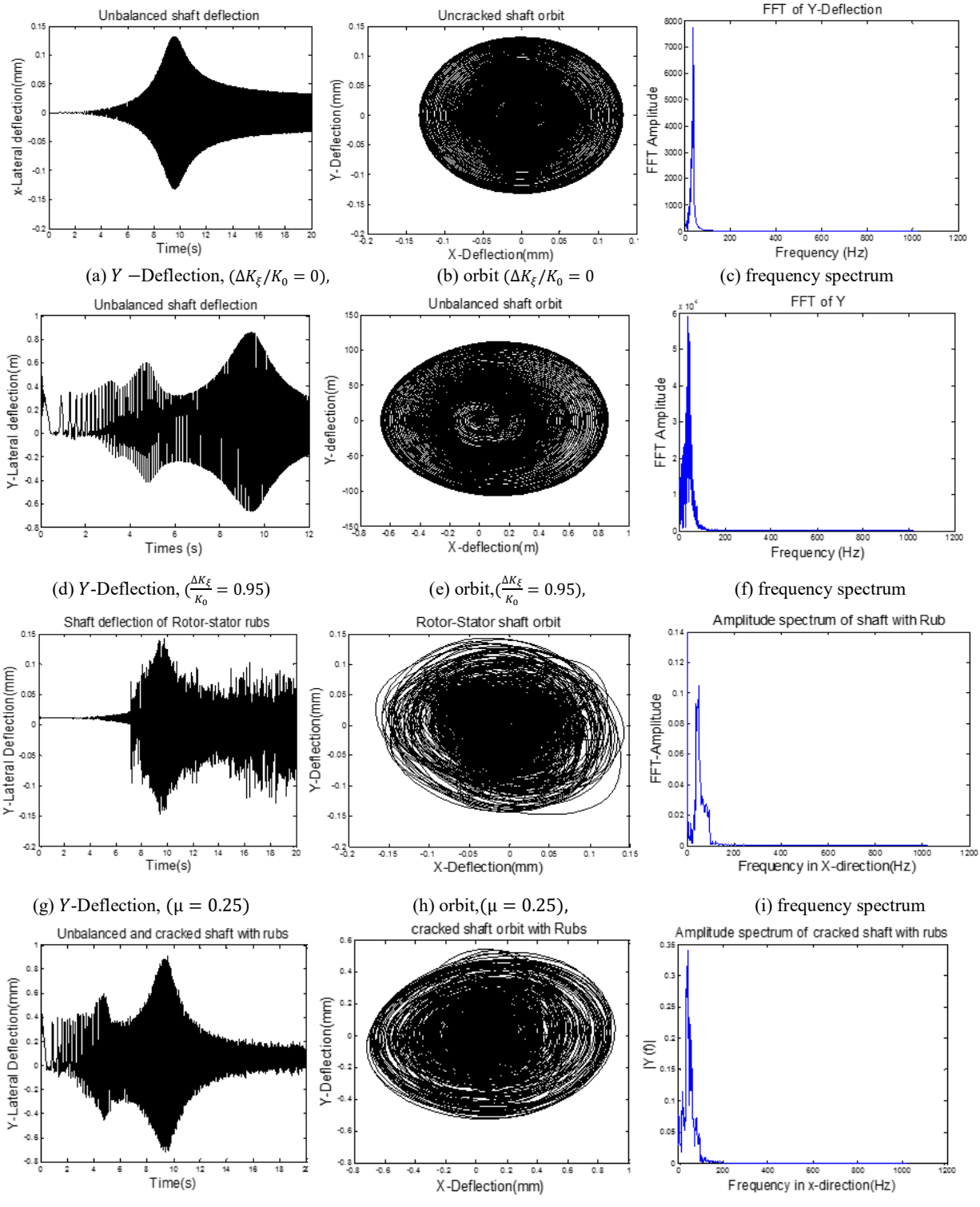

(a) Y −Deflection, $(\Delta K_\xi/K_0 = 0)$, (b) orbit $(\Delta K_\xi/K_0 = 0$ (c) frequency spectrum

(d) Y-Deflection, $(\frac{\Delta K_\xi}{K_0} = 0.95)$ (e) orbit,$(\frac{\Delta K_\xi}{K_0} = 0.95)$, (f) frequency spectrum

(g) Y-Deflection, $(\mu = 0.25)$ (h) orbit,$(\mu = 0.25)$, (i) frequency spectrum

(j) Y −Deflection,$(\mu = 0.25, \frac{\Delta K_\xi}{K_0} = 0.95)$ (k) orbit,$(\mu = 00.25)$ (l) frequency spectrum

Fig. 3 Dynamic response of rotor at low rotor's acceleration with unbalance, rubs, crack faults, passing through its first critical speed in time domain

Figs. 3 (d)-(f) show an increase in amplitudes of vibration in orbit analysis and rotor response, with the cracked rotor compared to the uncracked rotor at its first critical speed (at t=10s). The elliptical orbit observable in Fig. 3 (e) is now an oval curvature due to friction and the presence of crack. Moreover, observation of the vertical deflection in Figs. 3 (a), (g), and (j) shows that there is large increase in vibrations near the rotational speeds at one-half of the first critical speed (at t=5s).

Fig. 3 illustrates evolutions of the orbital patterns of the unbalanced rotor with rubbing occurrence and a breathing crack while passing through one-half of the first critical speed. It is observed that presence of a transverse breathing crack induces a loop containing multiple tightened loops inside Fig. 3 (e). It is noted that, the interaction between rotor and stator results in numerous irregular impact or rebounds in the orbit, which converges almost to the chaotic state as seen in Fig. 3 (h). These observations agree with reported simulations in [7].

A combination of unbalance, breathing crack, and rubs in Figs. 3 (j)-(l) presented a significant domination of crack features with some noise peaks related to the irregular contacts of the rotor with the stator. Presence of noise during the regular contact is identified by a multitude of peaks observed in the vibration responses (lateral displacement) in Fig. 3 (g); the peaks are present even in the combination of both rubs and crack as observed in Fig. 3 (j). Analysis of the orbit in Fig. 3 (k) shows that, contacts are not clearly detectable because of the nonlinearity of the stiffness. Therefore, the effects of crack presence overtake the effects of rotor-stator interaction. It is noticed from the frequency analysis in Figs. 3 (f) and (l) that frequency amplitude increases considerably when crack is open and it decreases considerably during the contact of rotor-stator as in Fig. 3 (l). As already illustrated in [7] the effect of a crack presence in Fig. 3 (l) overtakes again on frequency analysis features by increasing the shape and the amplitude at the resonance, in other words, the response frequencies differ somewhat.

The variation of amplitude responses observed in each different case at one-half of the rotor critical speed can be used to diagnose the fault in a rotor system at low rotor accelerations.

In order to illustrate the influence of the speed in the system and the difficulty of analysing the system using the spectral analysis; examination of the bearing model at high acceleration is shown in Fig. 4.

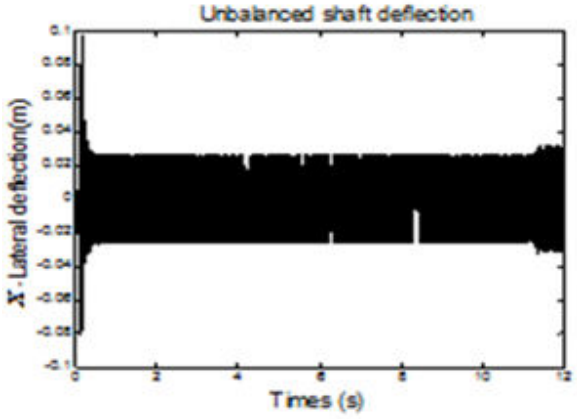

(a) X Deflection, $(\Delta K_{\xi}/K_0 = 0)$,

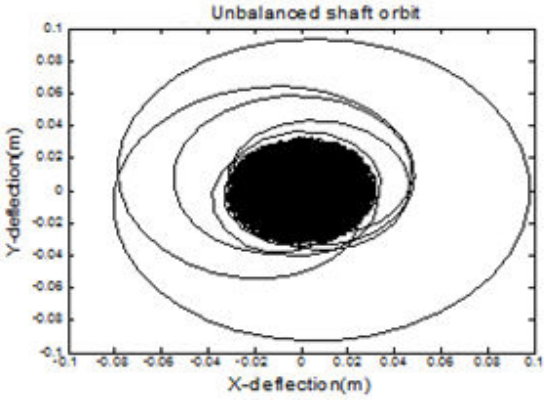

(b) Orbit $(\Delta K_{\xi}/K_0 = 0)$

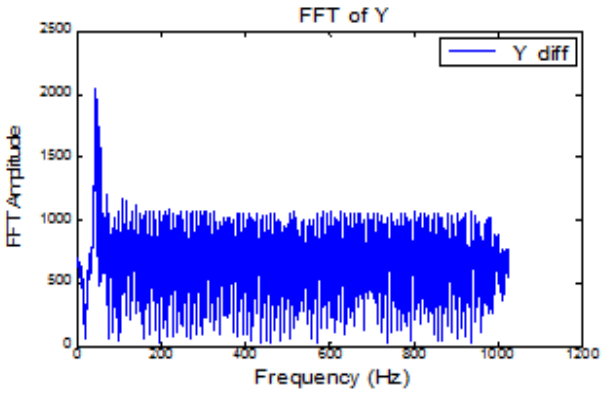

(c) Frequency spectrum

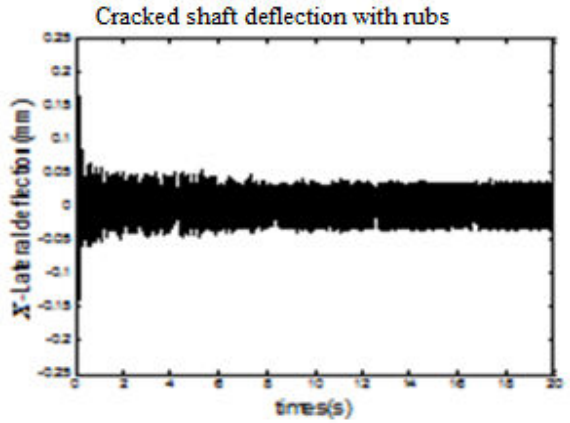

(d) XDeflection,$(\mu = 0.25, \frac{\Delta K_\xi}{K_0} = 0.95)$

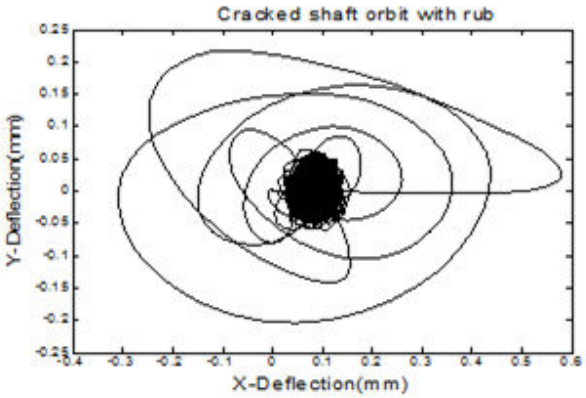

(e) Orbit,$(\mu = 00.25), \frac{\Delta K_\xi}{K_0} = 0.95$

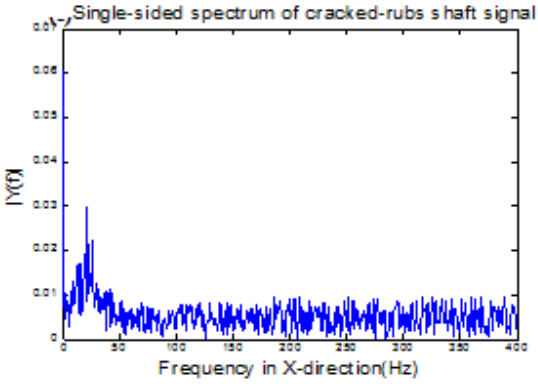

(f) Frequency spectrum

Fig. 4 Dynamic response of rotor with unbalance, rub and crack

It is clearly seen, that at low acceleration $a = 15\, rad/s^2$, Figs. 3 (c), (f), (i), and (l) the FFT peaks are more conspicuous than the FFT spectrum at high acceleration, $a = 150\, rad/s^2$, (Figs. 4 (c) and (f)). It is also noted in Figs. 4 (b) and (f) that, the orbit patterns are quite disorderly compared to the orbits in Fig. 3. Therefore, faults are no longer diagnosable for larger values of a and analysis gives erroneous results.

However, for high values of the acceleration, the nonlinearities lead to a significant reduction of both the lateral deflection and the sup-harmonic response frequency over the whole frequency range (Fig. 4), i.e. the characteristic rotor fault frequency is not clear from the frequency spectrum. Although, there can be other explanations for the shift of the frequency ratio, the results in show that the influence of the higher acceleration and non-stationary behaviour have to be considered as a possible explanation of the simulated behaviour.

Based on the results observed in Fig. 4, the monitoring and identification of the mass unbalance and the rotor fault for high acceleration using the spectral analysis is difficult due to the non-stationary. Therefore, faults are no longer diagnosable for larger values of acceleration and analysis gives erroneous results. In this case, the conventional Fourier analysis provides a poor representation of signals localized in time. So, the evolutions of the classic spectrum cascade plots cannot be used for analyzing vibration characteristics of the model. Therefore, the WT will be applied to the vibration signals to diagnose the fault.

VIII. Analysis by Continuous Wavelet Transform

The CWT has been performed at a low acceleration $a = 15\, rad/s^2$using the Daubechies wavelet of order 35, 'db35'with filter length of 70, as in [13]. At high acceleration, $a = 150\, rad/s^2$the Morlet wavelet algorithm [14] was used. Subsequently, the result of 'db35' decomposition of the vibration signal of mass unbalance, crack, and rubs sampled at a rotation speed of 143.3 $rpm.s^{-1}$ is given in Fig. 5.

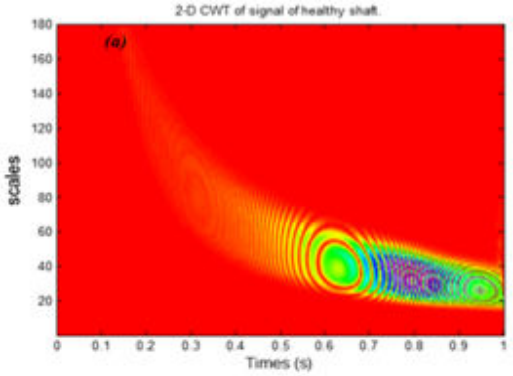

(a) C.W.T, of rotor with unbalance fault

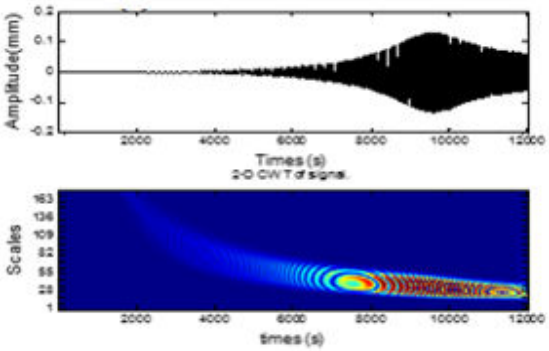

(b) Scalogram of healthy rotor

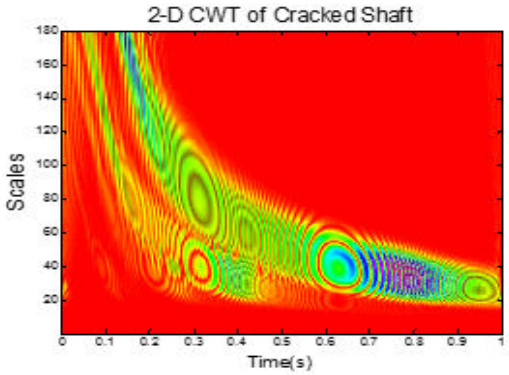

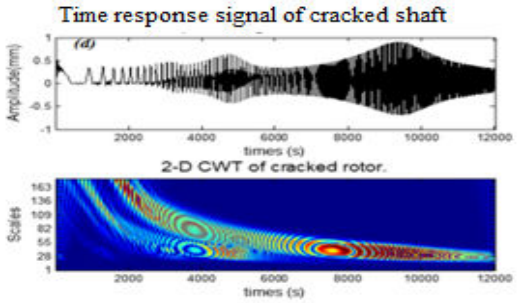

(d) Scalogram of cracked rotor ($\Delta K_\xi / K_0 = 0.5$)

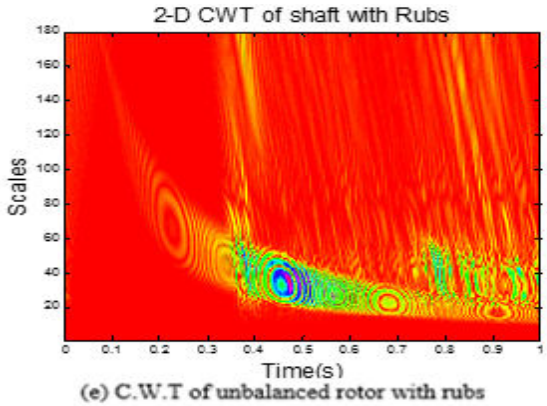

(e) C.W.T of unbalanced rotor with rubs

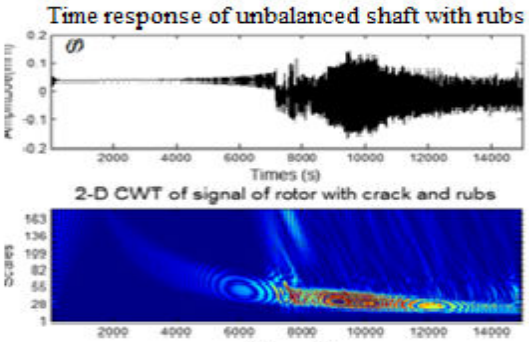

(f) Scalogram of rotor with rubs ($\mu = 0.25$)

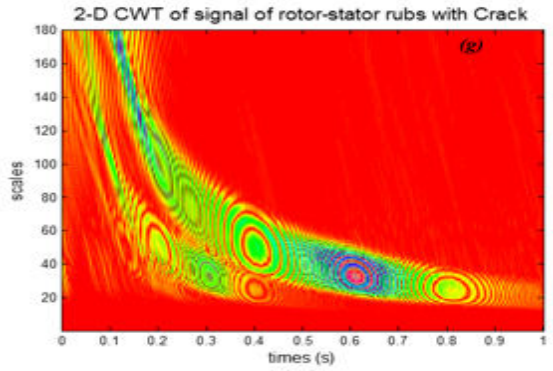

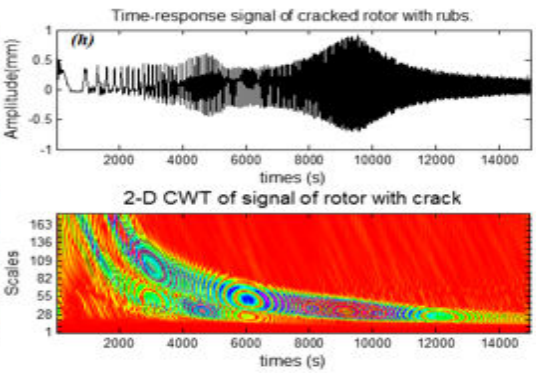

(g) C.W.T of unbalanced rotor with rubs and crack

(h) Scalogram, of unbalanced rotor with rubs and crack ($\Delta K_\xi / K_0 = 0.95$)

Fig. 5 Continuous Wavelet and power spectrum of the rotor with unbalance, crack, and rubs (with an acceleration of $a = 15\ rad/s^2$)

The simulations are realized for the rotor system with and without faults for low rotor acceleration ($a = 15\,rad/s^2$). Fig. 5 shows the CWT coefficients and the corresponding scalogram energy for each wavelet coefficient for normal condition (unbalanced rotor) and disturbed condition all obtained in x direction (vertical).

In Figs. 5 (a) and (b), the plots show clearly the variation spectrum related to unbalanced rotor during passage via critical speed. The zone of large concentration in the energy distribution is located most of the time around the first critical speed (t=10000s), observed in Fig. 5 (b). Therefore, there is always a fine variation grid around this zone, characterizing specifically the type of fault parameter in the model. Therefore, the CWT run-up enables by the distribution of energy at the first and second half critical speed, the identification the presence of a transverse crack. Indeed, in Figs. 5 (c) and (d) the distribution energy of wavelet power spectrum in the direction of scale or frequency shows a high concentration of energy that corresponds to the sub-harmonic resonance of the cracked rotor.

It clearly appears in Figs. 5 (c) and (d) that, the presence of a transverse crack induces the appearance of a second maximum value of the normalized wavelet power spectrum at the passage to one-half the first critical speed (for $t \in [0.2-0.7]\ s$ or $t \in [4000-10000]\ s$ Figs. 5 (c), and (d)).

To explore the effectiveness of the rubs detection via the CWT, the associated normalized wavelet power spectrum is given in Figs. 5 (e) and (f). It clearly appears that there is significant change in performance of the detection of rubs via the continuous wavelet transform. At the first critical speed of the rotor, the normalized wavelet power spectrum energy increases with multiple peaks indicating the presence of rubbing effect in the rotator-stator system. In Figs. 5 (g) and (h) the wavelet power spectrum consists of both rubbing and crack effects. From Fig. 5, it appears that there is no significant change in performance of the detection of rubs in presence of transverse crack via the CWT. The crack effects once again predominate as observed in Fig. 3 (l).

From the above analysis, CWT has been useful on vibration system analysis containing mass unbalance, crack, and rubs, both combination of rubs and crack. Better results in Fig. 5 are obtained by identifying the various types of faults. Such method is therefore useful for improving the condition monitoring and faults diagnosis of rotating machines.

In the case of the vibrating system operating under high variable speed conditions, for non-stationary signals, both the frequencies and their magnitudes vary with time as seen in Fig. 6. Thus, the conventional Fast Fourier Transform does not provide sufficient diagnostic information.

The CWT is now performed using the Morlet wavelet and Daubechies wavelet to analyze the non-stationary inputs and responses of the rotor fault vibration system at a high acceleration ($a = 150\,rad/s^2$) .

Fig. 6 shows the 2-dimension and 3-dimension scalograms of rotor under variable excitations parameters, which were obtained from the CWT by using Morlet family. Analysis of Figs. 6 (a) and (b), shows that, the vibration energy of the unbalanced rotor has been greatly restrained by a multiple breakdown point, which occurs after each consecutive period of $t = 0.4 \times 10\text{^}4s$. Similar time frequency traits can be seen in Figs. 6 (a), (c), (e), and (g).

The vibration energy of the rotor system at the passage into the resonance frequency region is observed at the startup and represented in Figs. 6 (b), (d), (f), and (h) by several compressed crests.

Fig. 6 (b) shows the presence of the high peak related to the second sup-critical speed, which appears clearly in the 3-dimension plot of scalogram result of CWT. In the graphic of the observed coefficients modulus, high modules in red showed the fault evolution on the increased value from 0.2 to 0.4 coefficients. Essentially, the features initially observed in the evolutionary power spectrum are depicted with more detail when change occurs on that reference graph in Figs. 6 (a) and (b).

The signal of cracked rotor (Figs. 6 (c)-(d)) is observed over relatively short periods. The apparent breaking point peaks observed in the evolutionary power spectrum Figs. 6 (a) and (b) does not appear identically on the cracked rotor's wavelet spectrum. It seems disturbed by the opening and closing of the transverse crack. In contrast, it reveals the existence in Figs. 6 (e) and (f) of a complex structure over the time interval, characterized by many equivalent red peaks when rub is introduced at almost the same amplitude, the position of each peak oriented on the interval period of shock equal to $t = 0.4 \times 10\text{^}4s$.

Once again, the combination of the crack and the friction on the vibratory system has a slight dominance of crack features on the scalogram of Figs. 6 (g) and (h). It can also be observed, the presence of a compressed mesh peak characterizing the interaction of the rotor and stator. As seen the vibration energies of the system are getting bigger for non-stationary signal, their frequency bands are getting broader in the friction process analysis Figs. 6 (e) and (f) and the fault energy evolution on the increased value when the crack is introduced Figs. 6 (g) and (h).

From the above findings, the technique based on WT is currently an advantageous tool to study time-series produced by non-stationary dynamical systems. CWT has provided with high accuracy the time-frequency map of transient “energy flow” of the unbalanced rotor with transverse crack and rubs in the rotor vibration system. Thus, the WT may be used in rotor vibration system, to provide more results that are reliable.

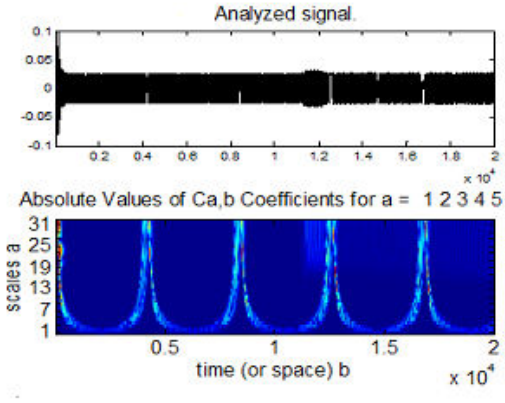

(a) Time-frequency of unbalanced rotor

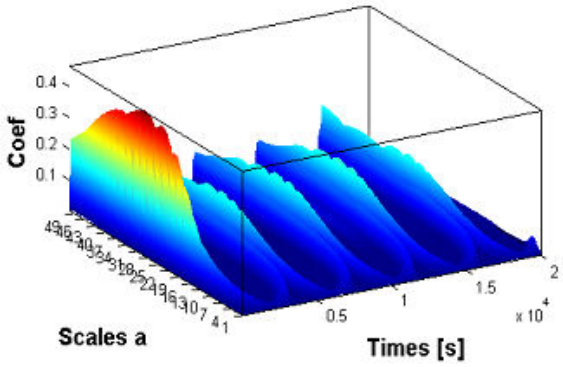

(b) Morlet Complex Wavelet of unbalanced rotor

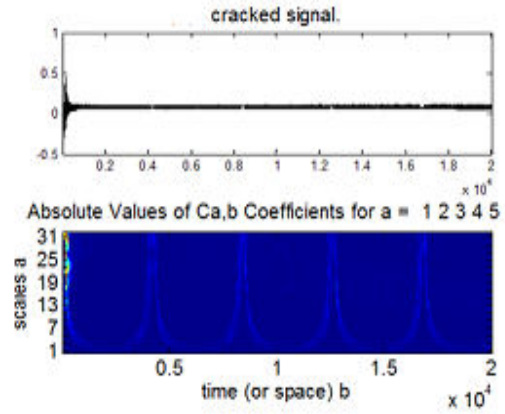

(c) Time-frequency maps of cracked rotor

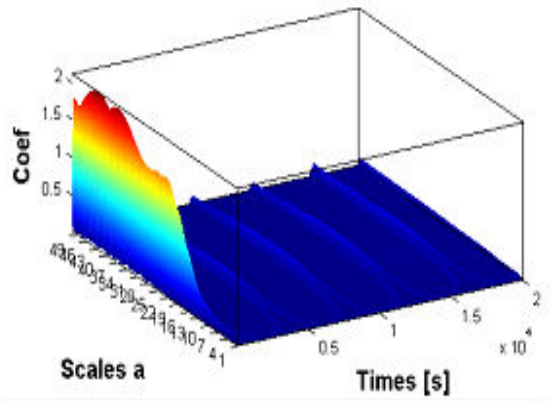

(d) Morlet Complex Wavelet of cracked, unbalanced rotor

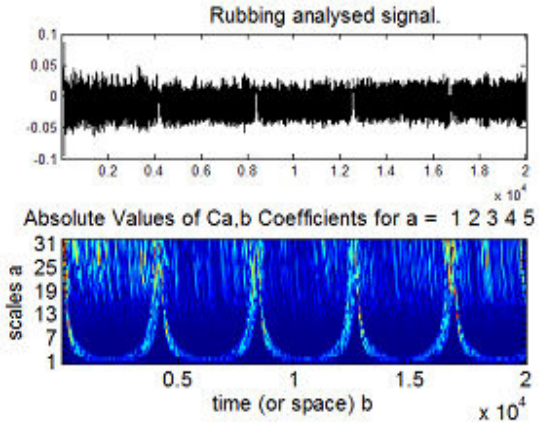

(e) Time-frequency of rotor with rubs

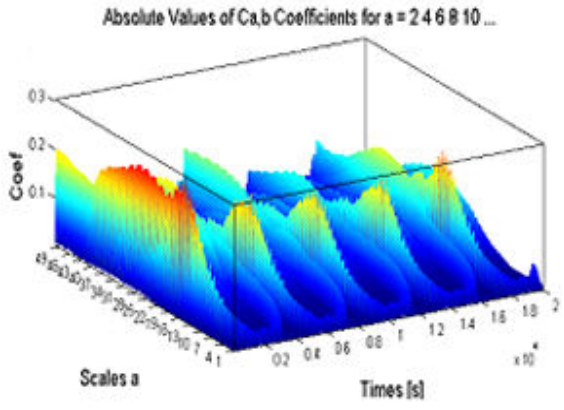

(f) Morlet Complex Wavelet of rotor with rubs

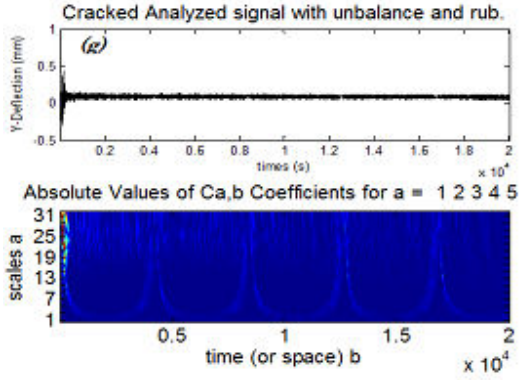

(g)Time-frequency of cracked rotor with rubs

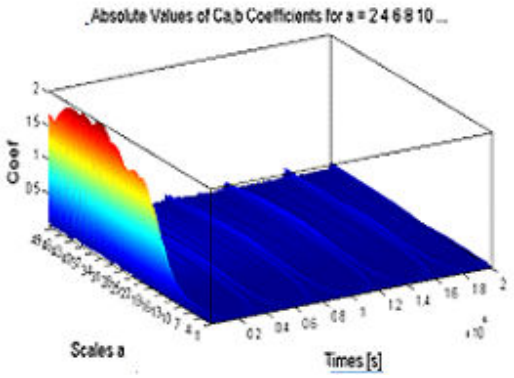

(h) Morlet Complex Wavelet of cracked rotor with rubs

Fig. 6 2-D and 3-D scalograms result from CWT under high variable speed conditions$a = 150\ rad/s^2$

IX. Conclusion

This paper has investigated the detection of damaged rotor using the simplified dynamic model of an extended cracked Jeffcott-rotor, supported on journal bearings, with a crack at or near its shaft mid-span, and regularly getting, several contact effect with fixed stator. Both fast Fourier transform (FFT) for rotor operating at low acceleration with multiple faults (crack, rub, unbalance), and wavelet analysis for low and high acceleration have been used for analysis in the rotor-stator system. For steady-state vibration (low rotor's accelerations), the spectrum plots of the power spectral density and orbits loops can be useful to detect the presence of rubs and open cracks. Better results are obtained by identifying the type of fault with CWT. WT methods clearly exhibit a local representation of the non-stationary rotor signals. Analyzing the energy of some wavelet decompositions is the powerful way to extract useful features of a cracked rotor with and without rub forces. The results of time-frequency characteristic of cracked rotor with rubs by Morlet wavelet indicate that the WT can diagnose the abnormal change in the measured data efficiently for fault detection purpose. Finally, it may be stated that the wavelet transform has been successfully used for the detection of faults, and is especially suitable for non-stationary vibration signal. Therefore, WT is useful for improving the conditions monitoring and mixed-faults diagnosis of rotating machines.

Acknowledgment

Support by the Department of Mechanical Engineering, Vaal University of Technology towards this work is highly acknowledged by the authors.

References

[1] A. S. Sekhar, Crack identification in a rotor system: a model- based approach. Journal of sound and vibration 270, 2004, 887-920.
[2] R. Gasch, IMechE Conference Publication c178/76, 1976, 123-128. Dynamic behavior of a simple rotor with cross-sectional crack.
[3] A. D. Dimaragonas and C. A. Papadopoulos, Journal of Sound and Vibration 91, 1983, 583-593. Vibration of cracked shafts in bending.
[4] C. A. Papadopoulos and A. D. Dimaragonas, Journal of Sound and Vibration 117, 1987, 81-93. Coupled longitudinal and bending vibrations of a rotating shaft with an open crack.
[5] M.I. Friswellc, J.K. Sinhaa, A.W. Leesb, Journal of Sound and Vibration 272 (2004) 967–989. Estimating unbalance and misalignment of a flexible rotating machine from a single run-down.
[6] A. S. Sekhar, and B. S. Prabhu, Condition monitoring of cracked rotor through transient response, 1998 Mech. Mach. Theory 33, 1167-1175.
[7] B.X. Tchomeni, A.A. Alugongo, L.M. Masu, In situ Modelling of Lateral-Torsional Vibration of a Rotor-Stator with Multiple Parametric Excitations. World Academy of Science, Engineering and Technology International Journal of Mechanical, Aerospace, Industrial and Mechatronics Engineering Vol: 8 No: 11, 2014.
[8] B. O. Al-bedoor, Transient torsional and lateral vibrations of unbalanced rotors with rotor-to-stator rubbing. Journal of Sound and vibration 229(3), 2000, 627-645.
[9] R. Sukkar, and A.S. Yigit, Analysis of fully coupled torsional and lateral vibrations of unbalanced rotors subject to axial loads. Kuwait J.Sci.Eng.35 (2B), 2008, pp. 143-170.
[10] J.-J. Sinou, "An experimental investigation of condition monitoring for notched rotors through transient signals and wavelet transform" 2009.
[11] S. Prabhakar, A. S. Sekhar and A. R. Mohanty, Mechanical Systems and Signal Processing 15, 2001, 447-450. Detection and monitoring of cracks in a rotor-bearing system using wavelet transforms.
[12] A. A. Alugongo, A dual Time-Frequency-Feature investigation and diagnostics of a cracked de-Laval rotor. IEEE AFRICON 2009.
[13] I. Daubechies, "Orthonormal bases of compactly supported wavelets," *Communication on Pure and Applied Mathematics*, vol. 41, pp. 909-996, 1988.
[14] S. Mallat, A wavelet Tour of Signal Processing, Academic Press, San Diego 1998.